CONF-951182--2
SAND95-1873C

Ion Divergence in Magnetically Insulated Diodes

S. A. Slutz, R. W. Lemke, T. D. Pointon, M. P. Desjarlais, D. J. Johnson, T. A. Mehlhorn, A. Filuk, and J. Bailey

Sandia National Laboratories, Albuquerque, N. M. 87185-1186

abstract

Magnetically insulated ion diodes are being developed to drive inertial confinement fusion. Ion beam microdivergence must be reduced to achieve the very high beam intensities required to achieve this goal. Three-dimensional particle-in-cell simulations [Phys. Rev. Lett. 67, 3094, (1991)] indicate that instability induced fluctuations can produce significant ion divergence during acceleration. These simulations exhibit a fast growing mode early in time, which has been identified as the diocotron instability. The divergence generated by this mode is modest due to the relatively high frequency (>1GHz). Later, a low-frequency low-phase-velocity instability develops. This instability couples effectively to the ions, since the frequency is approximately the reciprocal of the ion transit time, and can generate unacceptably large ion divergences (> 30 mrad). Linear stability theory reveals that this mode requires perturbations parallel to the applied magnetic field and is related to the modified two stream instability. Measurements of ion density fluctuations and energy-momentum correlations have confirmed that instabilities develop in ion diodes and contribute to the ion divergence. In addition, spectroscopic measurements indicate that the ions have a significant transverse temperature very close to the emission surface. Passive lithium fluoride (LiF) anodes have larger transverse beam temperatures than laser irradiated active sources. Calculations of source divergence expected from the roughness of LiF surfaces and the possible removal of this layer is presented.

PACS 41.80.Gg, 52.25.Wz, 41.80.-y

I. INTRODUCTION

Intense light ion beams are being developed to drive inertial confinement fusion (ICF)[1]. It has been estimated[2] that the ion divergence must be reduced from the present value of approximately 20 mrad to a value of only 6 mrad. Therefore understanding the mechanisms that generate ion divergence is critically important.

Light ion beams can be efficiently produced by magnetically insulated diodes, which are driven by an electrical pulse from a pulsed power generator. A strong magnetic field transverse to the anode-cathode gap inhibits electron flow across the gap. Three dimensional (3-D) particle-in-cell (PIC) simulations using the code QUICKSILVER[3,4] have been used to study the divergence generated in these diodes[5-7]. In the simulations, electrons stream into the diode along the magnetic field lines and form an electron sheath between the virtual-cathode located at x_{vc} and the edge of the sheath located at x_*, see Fig 1. The virtual-cathode is defined by the magnetic flux surface closest to the anode that intersects the cathode. The electric potential on this flux surface should be near the cathode potential, since electrons can flow freely from the cathode along this flux surface. This is also true of all of the other field lines that intersect the cathode at positions further from the anode. Therefore, the electric field should be approximately zero between the virtual-cathode and the gas cell, which we refer to as the charge-neutral region. Initially the virtual cathode position is coincident with the physical cathode, i.e. $x_{vc}=0$. A current is generated by the electrons flowing primarily in the **ExB** direction, which pushes the applied magnetic field toward the anode. This effect causes the dynamic gap g to decrease with a resulting increase in the ion current[8].

The large variation of the **E** field across the sheath results in considerable shear, which drives surface waves at the edge of the sheath labelled x_* and at the virtual cathode position, x_{vc}, where the electron density gradient is large. The interaction of these surface waves leads to a fast growing fluid instability[9] called the "diocotron". Transverse magnetic linear stability theory gives a good estimate of the initial growth rates[6,10] and a simple trapping model[5] yields a saturated amplitude for the mode that is in good agreement with the simulations. The frequency of this instability is rather high (greater than 10^9 Hertz) as compared to the reciprocal

of the ion crossing time and consequently, it does not generate a large ion divergence (<10 mrad). Its most important effect is to break the symmetry of the diode in the **ExB** direction, thus allowing electrons to cross the magnetic field toward the anode and thus broaden the gap. In section II, we present a stability analysis of a diode equilibrium model, which can closely approximate the various stages of the sheath development. We find that the growth rate of the diocotron instability decreases as the electron sheath is broadened as one would expect. The growth rate is also reduced when perturbations parallel to the applied magnetic field are included. Such perturbations could be induced by nonuniform ion emission or the onset of the ion mode. This may explain why the diocotron instability has not been observed experimentally on diodes using a lithium fluoride (LiF) ion source, which produces a nonuniform ion beam. It may also explain why the simulations show a rather abrupt transition from the diocotron mode to the low frequency ion mode, since the ion mode has structure parallel to the applied field.

In section III, we study the low frequency ion mode. The simulations indicate that during the diocotron phase the electron sheath broadens until it extends to the anode. This results in an increase in the ion current density and a transition to a low frequency instability, which has been termed the ion mode. The simulations indicate that this low frequency mode generates considerable ion divergence (>30 mrad). This is because the frequency is roughly equal to the reciprocal of the ion transit time, τ, and consequently an ion experiences only one half cycle of the wave as the ion crosses the accelerating gap. Higher frequencies do not produce ion divergence as effectively because the ion experiences many cycles of the wave as it crosses the accelerating gap and most of these cycles cancel each other out. Recently, a full mode set linear analysis[11] has revealed an unstable mode with a frequency and wavelength consistent with the ion mode observed in the simulations. This mode has structure parallel to the applied field, which is consistent with the simulation results. Section IV is devoted to strategies that could be used to reduce the ion divergence generated by the ion mode instability in magnetically insulated diodes.

Spectroscopic measurements[12] indicate that the ion beams have a significant divergence

very close to the source. In particular, the passive LiF generates a substantially larger divergence than the laser initiated plasma source, LEVIS. In section V, we discuss possible mechanisms that could generate the rather large source divergence generated by the LiF source. Finally, our conclusions are stated in section VI.

II. THE DIOCOTRON

A. Equilibrium

We assume a planer ion diode geometry as shown in Figure 1. This should cause little error since the accelerating gap is typically much smaller that the diode radius. Ions are injected at x=d and then accelerated by the electric field up to the virtual cathode at $x=x_{vc}$. The ions then drift unaccelerated through the charge-neutral region to the gas cell foil. The gas cell foil is assumed to be a conducting boundary and we restrict our analysis to the region between the anode and the gas cell. A large voltage, V, is applied across the gap resulting in an accelerating electric field (E~10 MV/cm). This electric field produces emission of ions from the anode and electrons from the cathode. A strong magnetic field, B_0~3 Tesla, is applied to the gap to inhibit the acceleration of electrons across the gap. The presence of both electric and magnetic fields results in an electron current in the ExB direction. As in previous work[13], we shall assume that the electron orbits are laminar. Thus the electron velocity is simply $v_{0e} = \frac{E_{0x}}{B_{0z}}$, where E_{0x} and B_{0z} are the self-consistent electric and magnetic fields. We shall assume that the electron density can be described as a simple function of the electric potential in the form $n(\phi) = n_0 + n_1\phi^{\alpha} + n_2\phi^{\beta}$. A simplified version of this model was used to study the early behavior of the numerical simulations[7]. In that case, the ions had not yet crossed the gap and the ion density could be neglected. A transverse magnetic (TM) analysis yielded growth rates frequencies and wavelengths in good agreement with the fluctuations seen in those simulations. Two of the parameters n_0, n_1, and n_2 are determined by the conditions that the electron and ion densities are equal in the charge-neutral region and the electron density is zero for $x > x_*$. The solution of Poisson's and Ampere's equations the boundary conditions, ϕ=V at the anode, and E=0 at the virtual cathode, determine the other parameter.

These equations can be used to determine all the equilibrium quantities needed in a linear stability analysis. Figure 2 shows electron density profiles calculated using this model with the parameters listed in table 1. These curves represent the various stages in the evolution of the electron sheath. The dotted curve is the electron density produced by a numerical simulation[7] (Fig. 20 curve labelled L1). We have included this curve for comparison with curve 3 of the equilibrium model. We have used the same parameters as in the simulation except for the voltage, which was 8 MV in the simulation. Electron density fluctuations, caused by the ion mode, result in most of the ion current coming from a relatively small area of the anode. We obtained better agreement with the simulations by reducing the diode voltage to compensate for this effect.

B. Linear stability

The diocotron instability generates the earliest fluctuations observed in the 3-D PIC simulations[5]. The diocotron instability is a fluid instability[9] driven by shear in the electron drift velocity. It results from the interaction of two surface waves, one at the virtual-cathode and one at the sheath edge. The fluctuations produced by these surface waves are strongest where the electron density gradient is the largest and decays exponentially from this point with a scale length $1/k_y$. Thus there is a maximum $k_y\delta x$ for unstable behavior, where δx is the sheath thickness. In the absence of fluctuations, the electrons would be confined to a thin sheath due to the strong applied magnetic field. Assuming conservation of energy and canonical momentum in the ExB direction one can easily obtain an expression for the thickness of sheath. The result is

$$\delta x = \frac{mc}{eB}\sqrt{\left(1+\frac{eV}{mc^2}\right)^2-1}\,. \qquad (1)$$

Note that this expression can be used to determine the critical insulating voltage of the diode by setting $\delta x=d$ and solving for $V=V_c$. In the presence of fluctuations, neither the energy nor the canonical momentum will be conserved. Indeed, the simulations show a time dependent broadening of the electron sheath once the diocotron instability turns on.

We use our equilibrium model to study the effect of this sheath broadening on the diocotron instability. We have performed stability analyses of the diode equilibria shown in Fig. 2, using the stability equations derived by Lemke and Slutz[11]. We have neglected ion perturbations since previous analyses[10] show that ion perturbations have virtually no effect on the diocotron instability, which is a pure electron mode. The results for k_z=0 are shown in Fig. 3. as solid curves labelled with the model number. As expected the diocotron growth rate is largest for the thinnest electron sheath, i.e. curve 1. As the sheath is broadened, curves 2 and 3, the maximum growth rate and the range of unstable growth is reduced, as we would expect from our previous discussion of the nature of the interaction of the two surface waves. Desjarlais[5] has made an estimate of the amplitude of the diocotron mode, $E_y \sim \omega_i B_0 (d+x_0)/\pi$, by assuming that the growth is saturated by trapping. Using this formula , the growth rate of curve 2 corresponds to the maximum amplitude of the diocotron mode, while the growth rate for curve 3 corresponds to the minimum amplitude, which occurs just before the transition to the ion mode. The simulations indicate that electron density profile evolves too quickly for the fluctuations to saturate at an amplitude consistent with the growth rate calculated from curve 1. Note that the phase velocity of the waves range from $v_{ph} \sim c/2.5$ to c/5, which is consistent with the simulations.

Ions are focussed onto a foil at the center of the applied-B diode that is fielded on **P**article **B**eam **F**usion **A**ccelerator **II** (**PBFA II**[1]). These ions are Rutherford scattered out of the beam into a magnetic spectrometer, which disperses the ions onto CR39 track recording film. According to Hamilton's equation, a given wave with phase velocity v_{ph} will cause the ions to disperse along a line in energy-momentum with slope $\frac{\Delta E}{\Delta P_\theta} = v_{ph}$. Desjarlais[14] showed that the magnetic spectrometer data exhibited this correlation. Results on diodes accelerating protons[6] indicate a phase velocity consistent with the diocotron mode early in the diode pulse.

Including perturbations parallel to the applied field decreases both the growth and the range of the instability as can be seen from the dotted curves in Fig. 3b. This suggests that nonuniformities in the direction parallel to the applied magnetic field will probably have a tendency to decrease the growth rate of the diocotron instability. This may explain why the

diocotron mode has been observed experimentally on diodes using a proton flashover source, but has not been observed when a LiF anode is used, since the LiF source is much less uniform than the proton flashover source.

III. THE ION MODE

The inclusion of ion perturbations has no significant effect on the diocotron mode when k_z=0. However, when $k_z > 0$, the inclusion of ion perturbations yields a new mode, which has been identified as the ion mode observed in the simulations[11]. This instability is essentially a modified two stream instability. The equilibrium model developed in the last section has been used to perform stability analysis of the ion mode. We found that the phase velocity of the mode decreases with increasing ion mass and increasing k_z. We also found that the growth rate increased with ion current density and decreased with injected ion velocity. This is consistent with a modified two stream instability, whose growth rate depends on the electron and ion densities. Unfortunately the stability equations are singular at points in the electron sheath where $\omega=k_y v_e(x)$. As the phase velocity of the wave decreases these singular points move toward the anode and the virtual-cathode making it very difficult to find numerical solutions to the equations for lithium ions at a significant k_z. The constant parameter model does not suffer from this difficulty[11] as long as the phase velocity of the wave does not equal the electron velocity. We use the constant parameter model to illustrate the stability of a lithium diode operating at moderate enhancement. The results of a calculation with the ion velocity equal to 0.02c, the electron drift velocity equal to 0.5c, the magnetic field times the gap equal to 2.5 T-cm, and the plasma frequency equal to 4.7c/d are shown in Fig 4. Notice that the peak growth occurs at increasing $k_y d$ as $k_z d$ is increased, but the real part of ω stays approximately constant, which is consistent with ion transit time resonance $\frac{\omega d}{c} = 2\pi\frac{v_i}{c} \approx 0.125$. This justifies our identification of this mode as the ion mode. The phase-velocity for k_z=2 is approximately c/20, which is typical of the phase velocities observed in the numerical simulations. The peak growth rate becomes negligible as k_z goes to zero, which explains why the numerical simulations have structure parallel to the applied field during the ion mode phase. Furthermore, the growth rate increases with beam density, which is consistent with the simulations, which typically exhibit

the transition to the ion mode at moderately high enhancement factors, J/J_{CL}.~7. However, when the ion density has axial nonuniformities, the transition to the ion mode occurs at significantly lower enhancement, J/J_{CL}.~2

The energy-momentum correlation indicates that the phase-velocity of the dominant waves in diodes using an LiF source are quite low (v_{ph}~c/30), which is consistent with the low phase velocity ion mode observed in the simulations[7]. The simulations also show that the ion beam density is modified by the presence of instabilities. We have measured the ion density fluctuations experimentally in an applied-B ion diode on the **PBFA-II**. Data from shot 6711, which used, a a passive lithium fluoride ion source is presented in Fig. 5. Voltages and currents are shown in Fig 5a. A small ion source was placed on the anode side of the magnetically insulated feed. The energy of these ions was used to determine the voltage at the diode, the solid curve. Ions generated by the beam are focussed onto a gold foil at the center of the diode. These ions are Rutherford scattered out of the beam and measured by three rows of PIN diode detectors in a magnetic spectrometer. The center row corresponds to no azimuthal deflection of the ion beam at the diode center. The rows to either side correspond to a change in the ion canonical momentum,. The center curve agrees reasonably well with diode voltage determined by the feed monitor . The left and right rows show a spread in beam energy of up to 1 MeV. The beam current was measured by charge-collection cups (Faraday cups). The cups were spaced at 7.5 degree intervals azimuthally in pairs both above and below the midplane of the diode. The ion current deduced from two cups at the same azimuthal position are plotted in Fig 5a. Notice that the two signals show maximal fluctuation when the left and right magnetic spectrometer voltages deviate from each other the most. Furthermore, the voltage measured by the right row is significantly above the diode voltage during maximum fluctuation. This behavior is expected from an instability and rules out charge-exchange as an explanation of the observed energy spread.

To study the fluctuations more closely we subtracted off the smoothed the signal. The results are shown in Fig. 5b. We have drawn a line through the points of maximum fluctuation from each curve. The change in azimuthal position with time indicates a phase-velocity of

approximately c/17. These curves clearly indicate that the wave is antisymmetric about the diode midplane indicating a nonzero k_z. The variation at 2 cm from the midplane was approximately the same as the data shown. Thus it is probable that the structure in z involves more than a single Fourier component. Inspection of Fig. 4, indicates a phase velocity of approximately c/17 at peak growth rate for $k_z d \sim 1.6$. This corresponds to an axial wavelength of approximately 8 cm, which consistent with the experimental data.

The magnetic spectrometer can also be used to estimate the beam divergence. The focussed beam was also Rutherford scattered into an instrument which we call the movie camera. The movie camera images this scattered beam onto an array of PIN diode detectors and can be used to determine the beam divergence as a function of time. The average of these two measurements is shown as the solid curve in Fig 5c, note that the divergence due to scattering in the gas cell foil has been removed. This is compared to the root mean square (r.m.s.) of the fluctuation amplitude measured by the Faraday cups shown as a dashed curve. Clearly there is a correlation between these two curves. The correlation would be more striking if the source divergence could be removed. Unfortunately this data is not available on this shot. On other shots values 15 mrad are typical for a passive lithium fluoride source.

IV. CONTROL OF DIVERGENCE CAUSED BY INSTABILITIES

We have identified several approaches that can reduce the divergence caused by instabilities. The simplest approach is to increase the degree of magnetic insulation. This decreases the ion current and delays or eliminates the transition to the ion mode. The degree of insulation is determined by the ratio V_c/V. The strength of materials limits the magnetic field strength that can be used. The ratio V_c/V can also be increased by increasing the accelerating gap or by lowering the voltage, however, this will also lower the beam intensity. Another approach is the use of an electron limiter[15] to keep the electron sheath from extending all the way to the anode. This keeps the electrons from the region where the ion density is largest and reduces the growth rate of the ion mode, which is a modified two stream instability. Numerical simulations[5] of ion diodes using electron limiters indicate that the transition to the ion mode

can be delayed indefinitely without high ratios of V_c/V. Furthermore, experiments on extraction diodes[16,17] have indicated improved ion divergence using a limiter. However, there is still some question as to whether a limiter will become a source of ions when the diode is operated at the high powers needed for a fusion driver.

The power on an ICF capsule should have a pulse length of approximately 10 ns. Since beam divergence is potentially the most serious weakness of the light ion approach, the final focus should be as close to the target as possible, say about 2 m. The diode could be located another 2 m from the final focussing lens. At 4 meters the beam could be bunched by approximately a factor of two, since the target cannot accept a large spread in ion energies. Thus the useful ion pulse at the diode is only about 20 ns. The present accelerators (e.g. PBFA-II) have beam pulse lengths of 40-50 ns and rather slow voltage rise-times of 20-30 ns. This slow voltage rise and long pulse give the electron sheath ample time to diffuse to the anode and enhance the ion current, with the resulting growth of the ion mode. A faster risetime shorter pulse accelerator could deliver the beam power before the ion mode has grown and thus at a much higher beam brightness. The results of three 3-D QUICKSILVER simulations are compared in Fig. 6. A singly charged lithium beam is accelerated across a 1.5 cm gap insulated by a 5 T magnetic field. The voltage risetime is 10ns for the solid curve, 20 ns for the dashed curve and 30 ns for the dotted curve. As can be seen the beam brightness is significantly higher for the faster risetime. In all of these cases the beam brightness would become larger later in time if the ion mode growth were suppressed. Therefore, it would be advantageous to also use a limiter, which may not be as prone to emitting ions with a shorter pulse. Plans are being made to test the fast rising pulse by installing a plasma opening switch on PBFA-II, which has been reconfigured to drive a magnetically insulated diode in extraction geometry, i.e. the beam is directed axially and the magnetic field is directed radially. Numerical simulations indicate that the transition to the ion mode takes longer and limiters work more effectively in the extraction geometry[18].

It has been shown both experimentally[19,20] and numerically[21] that ion divergence can be reduced by post acceleration of the beam. As in the single-stage simulations, the numerical

results indicate that the reduction occurs as long as the injected current density is not too large. However, the beam current density can be larger than in a single stage diode due to the injection velocity of the beam, which reduces the beam space-charge and thus the growth rate of the ion mode. Simulations indicate[21] that for sufficiently low injected beam current density there is no significant increase in the normalized emittance during post acceleration. Thus the divergence is reduced by increasing the longitudinal velocity.

A beam brightness of roughly 125 TW/(rad-cm)^2 is required to drive ICF capsules. Therefore it is probable that all of the techniques that we have described to lower divergence generated by instabilities will be needed. In addition, ion divergence can be generated by imperfections in the ion source, which we discuss in the next section.

V. SOURCE DIVERGENCE

Spectroscopic measurements of doppler broadened neutral lithium lines have been used to infer that the Li^+ ion beam has a significant transverse velocity spread within 50 μm of the anode source[12]. This effective *source temperature* depends on the ion source. The source temperature for the active laser initiated lithium source LEVIS was approximately 500 eV, while the passive LiF source temperature was approximately 1800 eV. Using the relation $\Delta\Theta = \sqrt{\frac{2\log 2 T}{V}}$, the divergence for the LEVIS source was inferred to be approximately 4-9 mrad assuming a diode voltage of 11 MV, while a divergence of approximately 15 mrad was inferred for the passive LiF ion source. Unfortunately, the spot size at the diode focus was nearly independent of the ion source used. This may be due to nonuniform emission of ion current from the LEVIS source. Nonuniform ion emission can produce significant ion divergence[22], when the scale length of the nonuniformities is several millimeters. Note that this mechanism would not produce significant divergence close enough to the anode to be detected by the spectroscopy. Furthermore, we do not have a diagnostic that can determine what the variation in ion current density is in the accelerating gap. The problem is that such variations will wash out by the time the beam reaches our diagnostics.

Stark shifted lines were used to determine the average electric field near the anode[23]. These results indicate that the electric field near the anode is approximately zero for the LEVIS source, as would be consistent for a preformed plasma, while the electric field is approximately 8 MV/cm for the passive LiF source. Apparently these sources operate by rather different mechanisms. It has been suggested by Tom Green[24] that the LiF emits Li^+ by electric field desorption. Surface roughness on a micron scale could potentially produce the source divergence that has been observed. The divergence generated by a rough surface or nonuniform plasma will depend on the electric field near the source. This may explain the larger source divergence observed with the LiF source. At the present we have no information about the roughness of the plasma generated by the LEVIS laser, so we will devote our attention toward understanding the divergence generated near the LiF source.

Atomic force microscopy and scanning electron micrographs show that the LiF layer is columnar with approximately 10^{10} columns/cm^2. Typically adjacent columns are nearly merged giving the surface a vertical relief of only 0.02 μm even though the LiF layer is 0.5-1.0 μm thick. We have used the technique developed by Y. Y. Lau[25] to estimate the divergence that ions would obtain when emitted from such a surface. The results are more than an order of magnitude too low to explain the spectroscopic data.

It has been found[26] that a LiF layer can be piecewise removed from tungsten tip at an electric field of approximately 6 MV/cm when the tip is at a temperature of 630 K. Estimates indicate that the LiF surface will be heated to approximately 700 K by electron bombardment in the PBFA-II applied-B ion diode and thus we might expect chunks of LiF to be removed from the substrate. Theory[24] predicts that LiF should become a reasonably good conductor when it is bombarded with electrons. Thus charges within a fragment will polarize to exclude the electric field. Assuming a spherical fragment the electric potential outside of the fragment will be given by the expression[27] $\phi = -E_0\left(r - \frac{b^3}{r^2}\right)\cos\theta$, where b is the radius of the fragment and E_0 is the background electric field. Taking the gradient of this potential we find that the electric field is three times the background on the surfaces that point toward and away from the anode. It seems likely that an electric field of 24 MV/cm will cause electrons to be emitted from the

side of the fragment that faces the anode. This could be due to a whisker explosion mechanism, as has been typically proposed for cold cathode emission, or it could be due to secondary emission of electrons from the high energy electrons bombarding the fragment. This process will charge up the fragment until the electric field on the surface facing the anode is zero. The potential is then given by

$$\phi = E_0\left(\left(r - \frac{b^3}{r^2}\right)\cos(\theta) - \frac{3b^2}{r}\right). \tag{2}$$

Taking the gradient of this expression, we find that the electric field is six times E_0 on the surface facing away from the anode, i.e. the field will be roughly 50-60 MV/cm. This is still smaller than the electric field necessary to cause field desorption from the most common sites of a LiF crystal.

Field desorption occurs because ions have a statistical probability of having an energy greater than the work function, which is lowered by an electric field at the surface. We can estimate the ion current from the expression

$$J = \frac{f_s}{a^3}\sqrt{\frac{kT}{M}}\exp\left(-\frac{E_M a}{kT}\left(1 - \sqrt{\frac{E}{E_M}}\right)^2\right), \tag{3}$$

where, T is the lattice temperature, $a=2\times10^{-10}$ m is the lattice spacing, M is the mass of a lithium ion, f_s is the fraction of the surface lithium ions with a given Madelung constant, A_M, and $E_M = \frac{eA_M}{4\pi\varepsilon_0 a^2}$. A typical LiF surface consists of large smooth regions known as terraces, which end in ledges. The end of the ledges are known as kinks. The Madelung constant for a kink site is roughly 0.85, while the value for an ion within the terrace is 1.7. We find from eq. (3) that the electric field needed to extract 1 kA/cm^2 is approximately 120 MV/cm for a kink site and is 320 MV/cm for a terrace site. Scanning electron micrographs suggest that the LiF crystal has rough structure down to tens of lattice spacings and thus microscopic fields at the ion emission sites may indeed exceed these values. We have numerically integrated the trajectories of ions leaving a fragment using the electric field derived from Eq. (2) and estimated the ion source temperature using Eq. (3) as a weighting function. Assuming the fragments have a radius of 1 μm, and $f_s=1$, we obtain a divergence of approximately 7-10 mrad. This is in rea-

sonable agreement with the spectroscopic results. Larger values are obtained by decreasing the Madelung constant or f_s. If the fragments are smaller the divergence scales as the square root of the fragment size and this mechanism would not produce as much divergence. If this scenario is correct, it is not obvious how LiF could be modified to reduce the source divergence. We are presently working on alternatives such as the LEVIS ion sources. The requirements of the ion source are a high degree of ion current density uniformity (< 10% variation of a scale length of a few millimeters) and low source temperature (T < 700 eV)

VI. Conclusions

Numerical simulations, analytic theory, and experimental data indicate that an unacceptably large ion divergence is generated by the ion mode instability. Theory and experiment indicate that operating the diode at high ion current densities compared the Child-Langmuir value causes a rapid onset of this ion mode. The ion current density can be controlled by maintaining a high degree of magnetic insulation, but this implies using a modest diode voltage or a large acceleration gap, both of which lower the beam brightness. The electron limiter can also control the diode current density with less restriction on the diode voltage and thus could potentially produce a brighter beam. However, the limiter may become a source of ions and cease operation as a limiter. We have also shown 3-D numerical simulations indicating that the beam brightness can be increased by reducing the voltage risetime. Furthermore, a short pulse combined with surface cleaning may keep a limiter from emitting ions during the power pulse. Fast rising voltage pulses will be tested experimentally by using a plasma opening switch. The beam can start with a significant temperature at the source, e.g. LiF has a transverse temperature of approximately 1800 eV. We need to develop an ion source of high purity and an ion temperature < 700 eV to obtain beams of sufficient brightness to drive ICF.

Acknowledgments: This work supported by U. S. Dept. Of Energy under Contract No. DE-AC04-94AL85000

References

1 J. P. VanDevender and D. L. Cook, Science **232,** 831 (1986).

2 C. Olson, 1988 Linear Accelerator Conf. Proc., CEBAF Report 89-001, June 1989, P. 34 (see National Technical Information Service document no DE90007862. Copies may be ordered from the National Technical Information Service, Springfield, Virginia 22161. The price is $73.00 plus a $3.00 handling fee. All orders must be prepaid.)

3 D. B. Seidel, M. L. Kiefer, R. S. Coats, A. L. Siegel, and J. P. Quintenz, "QUICKSILVER-A 3-D, electromagnetic, PIC code," in Proc. 12th Conf. Numerical Simulation of Plasmas, San Francisco, CA, paper PT_24, 1987

4 D. B. Seidel, M. L. Kiefer, R. S. Coats, T. D. Pointon, J. P. Quintenz, and W. A. Johnson, in *Computational Physics*, edited by A. Tenner (World Scientific, Singapore, 1991), pp. 475-482.

5 M. P. Desjarlais, T. D. Pointon, D. B. Seidel, R. S. Coats, M. L. Kiefer, J. P. Quintenz, and S. A. Slutz, Phys. Rev. Lett. 67, 3094 (1991).

6 J. P. Quintenz, M. P. Desjarlais, T. D. Pointon, S. A. Slutz, D. B. Seidel, T. A. Mehlhorn, R. S. Coats. M. L. Kiefer, N. A. Krall, L. D. Bacon, Proceedings of the IEEE, Special Section on Pulsed Power Technology, edited by J. P. VanDevender, **80**, 971-984 (1992).

7 T. D. Pointon, M. P. Desjarlais, D. B. Seidel, S. A. Slutz, R. S. Coats, M. L. Kiefer, and J. P. Quintenz, Phys. Plasmas 1, 429 (1994).

8 M. P. Desjarlais, Phys. Rev. Lett. **59**, 2295 (1987). and M. P. Desjarlais, Phys. Fluids B **1**, 1709 (1989).

9 O. Buneman, R. H. Levy, and L. M. Linson, J. Appl. Phys. **37**, 3203 (1966).

10 S. A. Slutz, and W. A. Johnson, Phys, Fluids B **4**, 1349 (1992).

11 R. W. Lemke, and S. A. Slutz, Phys. Plasmas 2, 549, (1995).

12 R. W. Stinnett, T. A. Green, D. J. Johnson, T. R. Lockner, T. A. Mehlhorn, J. E. Bailey, A. Filuk, and L. P. Mix: A. B. Filuk, J. E. Bailey, K. W. Bieg, A. L. Carlson, T. J. Renk, G. C. Tisone and Y. Maron, 9th International Conference on High-Power Particle Beams, Washington, D. C. 25-29 May 1992, edited by D. Mosher and G. Cooperstein (Naval Research Laboratory, Maryland, 1992), p. 788 and p. 794.

13 T. M. Antonsen, Jr. E. Ott, Phys. Fluids **19**, 52 (1976)

14 M. P. Desjarlais, Sandia National Laboratories, Albuquerque, N. M., personal communication.

15 S. A. Slutz, T. A. Mehlhorn, J. E. Maenchen, C. Ruiz, and J. R. Woodworth, J. Appl. Phys. **62,** 16 1987.

16 See National Technical information Service Document No. PB92-206168 (H. Bluhm, P. Hoppe, H. Bachmann, W. Bauer, K. Baumung, L. Burth, H. U. Karow, H. Laqua, D. Rusch, E. Stein, and O. Stoltz, *Proceeding of the 9th International Conference on High-Power Particle Beams*, Washington, D. C. May 1992, p. 51). Copies may be ordered from NTIS, Springfield, VA 22161

17 J. B. Greenly, C. K. Struckman, B. R. Kusse, and W. A. Noonan, ibid., p. 43

18 M. P. Desjarlais and T. D. Pointon, ibid., p. 775

19 S. Miyamoto, K. Yasuike, S. Nakai, K. Imasaki, and C. Yamanaka, ibid. , p. 884

20 T. Lockner, S. Slutz, J. W. Poukey, and W. A. Stygar, Proceedings of the IEEE, 9th International Pulsed Power Conference, Albuquerque, New Mexico, edited by B. Baker and K. prestwich (Institute of Electrical and Electronic Engineers, New York, 1993).

21 S. A. Slutz, J. W. Poukey, and T. D. Pointon, Phys. Plasmas, **1**, 2072, (1994).

22 S. A. Slutz, Phys. Fluids B 4, 26, (1992).

23 J. E. Bailey, A. B. Filuk, A. L. Carlson, D. J. Johnson, P. Lake, E. J. McGuire, T. A. Mehl-

horn, T. D. Pointon, T. J. Renk, W. A. Stygar, and Y. Maron, Phys. Rev. Letters, 74, 1771, (1995).

24 T. A. Green, R. W. Stinnett, R. A. Gerber, P. F. McKay, M. F. Lopez, R. A. Anderson, T. D. Pointon, L. J. Lorence, Jr. J. A. Halbleib, and A. B. Filuk, Production of Lithium Positive Ions from LiF Thin Films on the Anode in PBFAII, Sandia National Labs Report no. SAND95-1794, August 1995 (available from NTIS).

25 Y. Y. Lau, J. Appl. Phys. 61, 36 (1987).

26 J. A. Panitz, Synergistic studies of ion production from LiF thin films, Progress Report August,1993, Contract: AG-3854.

27 J. D. Jackson, Classical Electrodynamics, (John and Wiley, N.Y. 1962), p. 34.

Table 1: Parameters for the 3 curves in Fig. 2. The voltage is 7 MV, d_0 = 1 cm, d = 1.5 cm, B=3.5 T, and the ion is Li^+.

curve#	ϕ_*	α	β	J/J_{cl}
1	0.3	0.5	2.0	3.3
2	0.7	0.4	4.0	8.5
3	1.0	0.3	8.0	20.

Figure captions

1 A schematic of an Applied-B ion diode. The applied magnetic field is in the axial or z-direction.

2 Several electron density profiles as calculated from the equilibrium model are plotted. The parameters used for these curves are listed in table 1. The electron density profile from a 3-D PIC simulation is plotted (dotted line) for comparison.

3 The real (top) and the imaginary (bottom) values of $\omega d/c$ are plotted as a function of $k_y d$ for the three electron density profiles shown in Fig. 2. The solid curves are results with $k_z=0$. The dotted curves (bottom) show growth rates for the electron density profile 1 and are labelled with the value of k_z.

4 The real (top) and the imaginary (bottom) values of $\omega d/c$ are plotted as a function of $k_y d$. Ion perturbations and the complete mode set is used in the stability analysis. Each curve is labelled with the value of $k_z d$ used in the calculation. Equilibrium parameters are given in the text.

5 Data from PBFA-II are plotted as a function of time: a) The solid curve is the diode voltage, the dashed (dotted) [dash-dot] curve is the energy of ions on the center (left) [right] row of the magnetic spectrometer, the solid (dashed) curve is the ion current measured by a Faraday cup 4 cm above (below) the midplane; b) The solid (dotted) curves are ion current density fluctuations measured at various azimuthal locations by Faraday cups above (below) the midplane, each displaced by 2 kA/cm^2 to separate the curves. ; c) The experimentally determined beam divergence (solid) is compared to the r.m.s variation of the of the Faraday cup signals (dashed).

6 The beam brightness from three simulations are plotted as a function of time. The voltage risetimes were 10 ns (solid) , 20 ns (dashed) , and 30 ns (dotted).

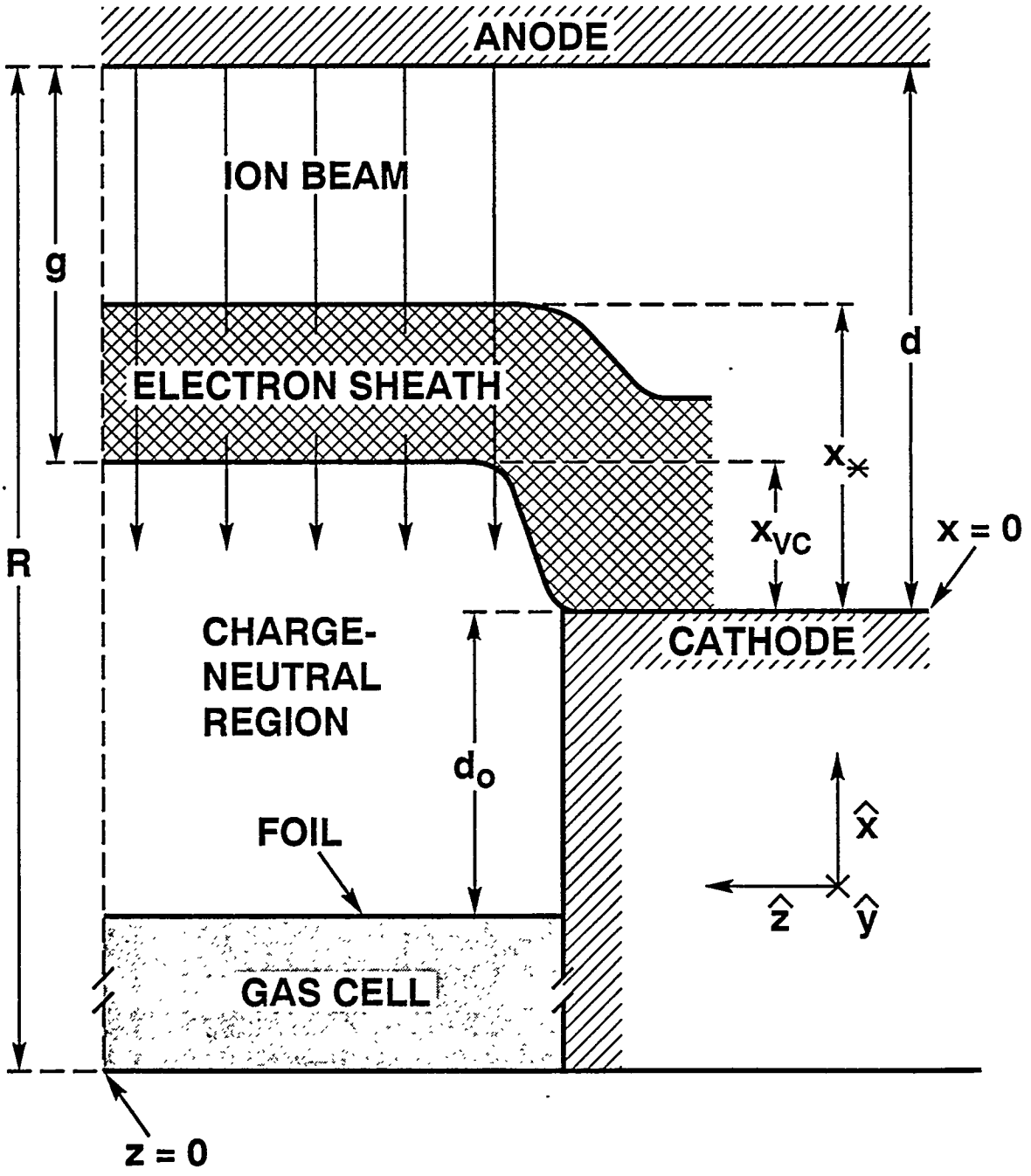
ANODE
ION BEAM
g
d
ELECTRON SHEATH
x_*
x_{VC}
x = 0
R
CHARGE-
NEUTRAL
REGION
CATHODE
d_o
FOIL
$\hat{x}$
$\hat{z}$
$\hat{y}$
GAS CELL
z = 0

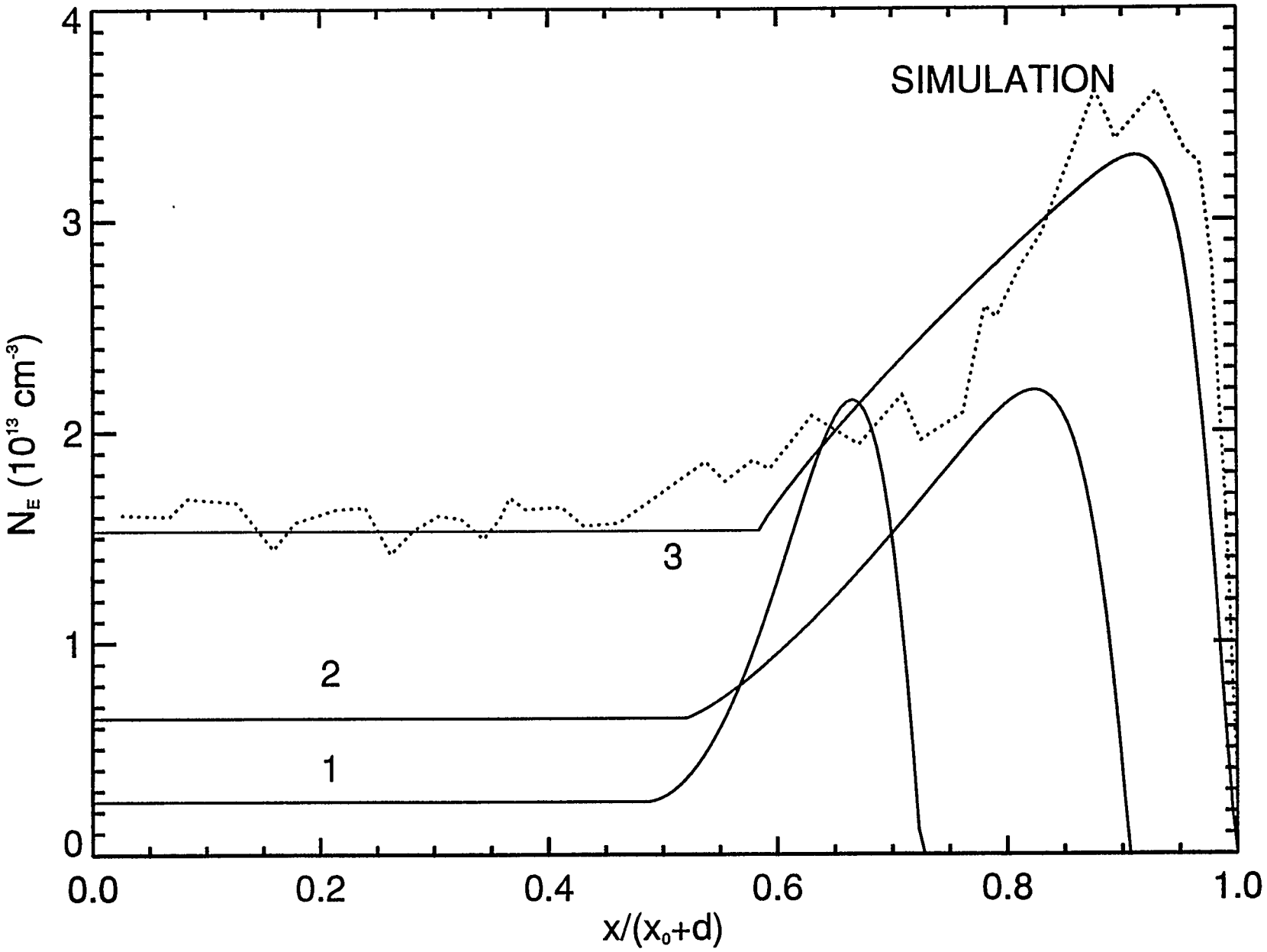
SIMULATION
3
2
1
N_E (10^{13} cm^{-3})
$x/(x_0+d)$
0
1
2
3
4
0.0
0.2
0.4
0.6
0.8
1.0

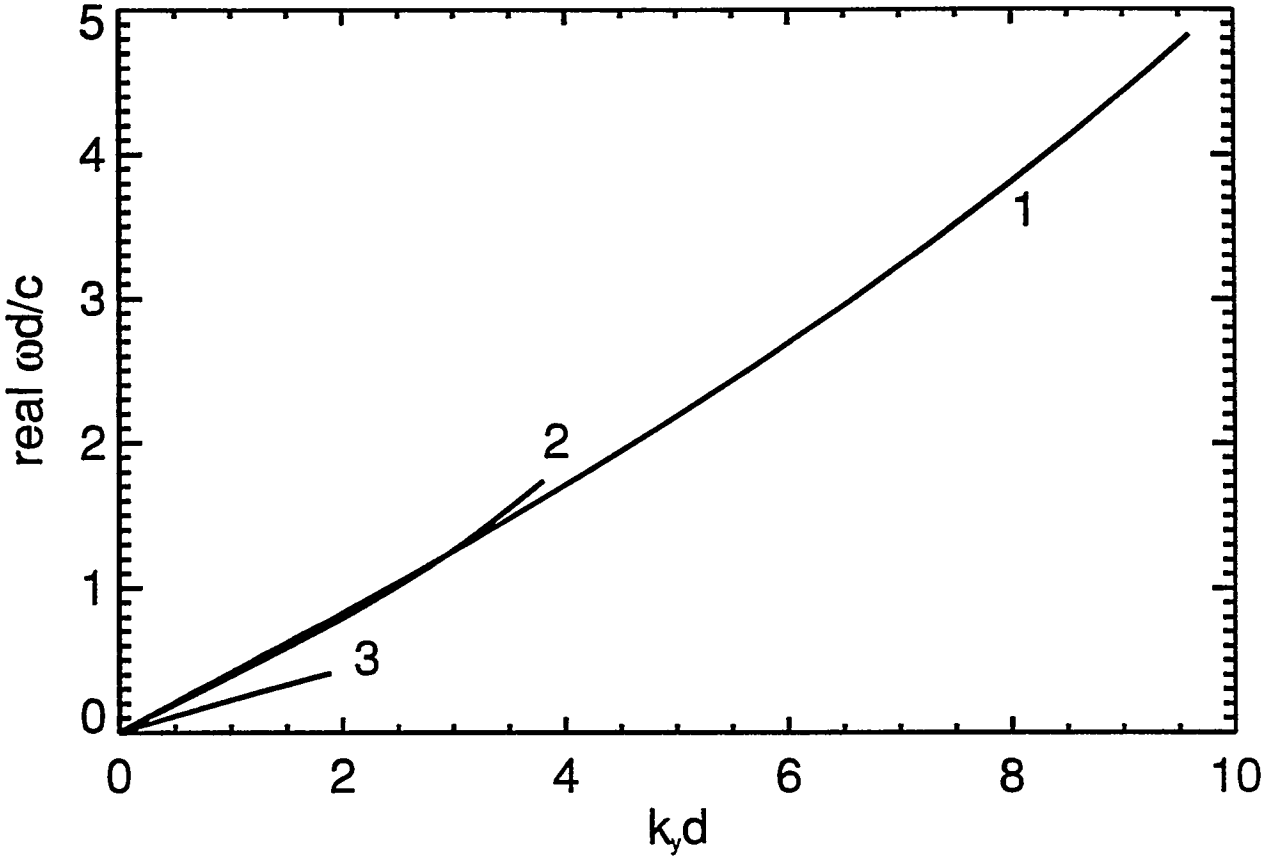
real ωd/c
k_y d
1
2
3

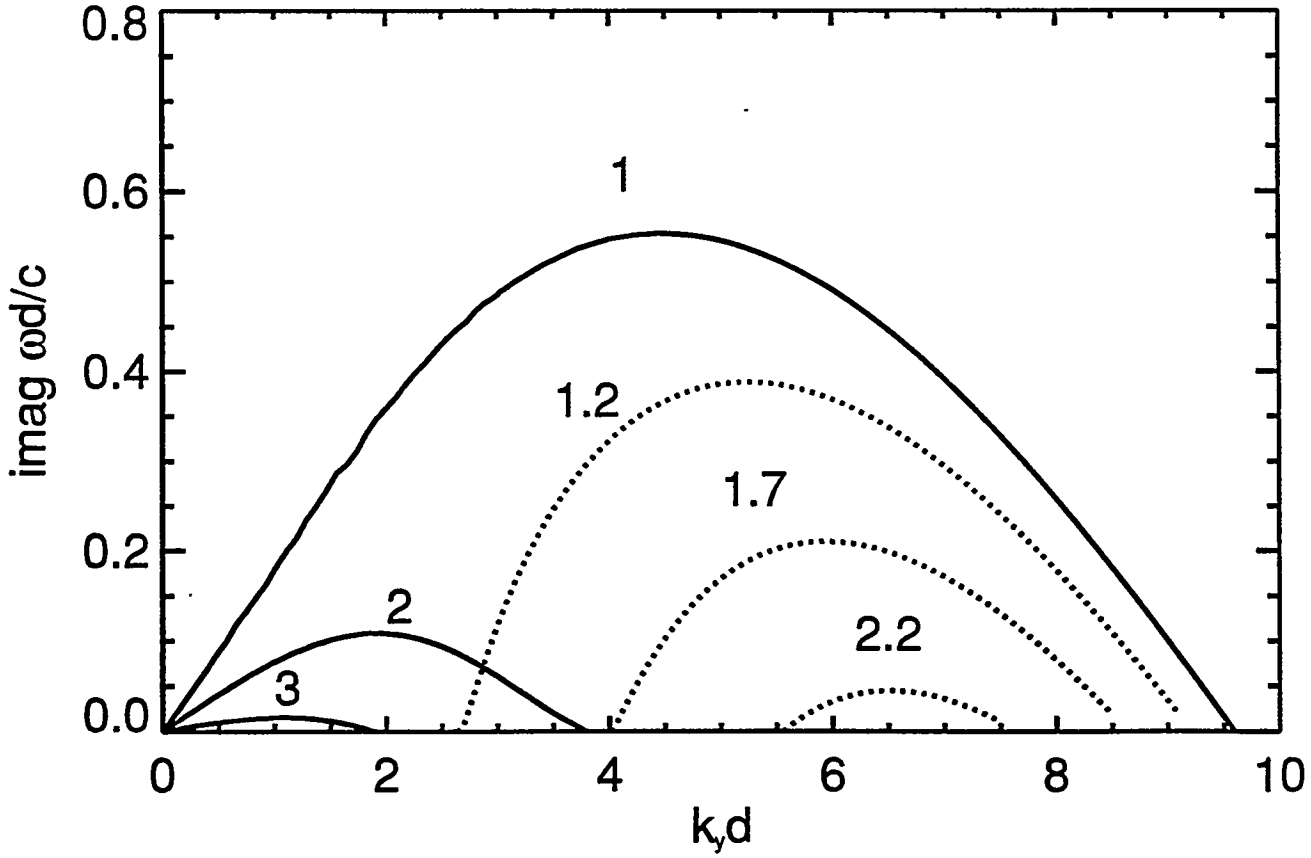
imag ωd/c
k_y d
1
1.2
1.7
2.2
2
3

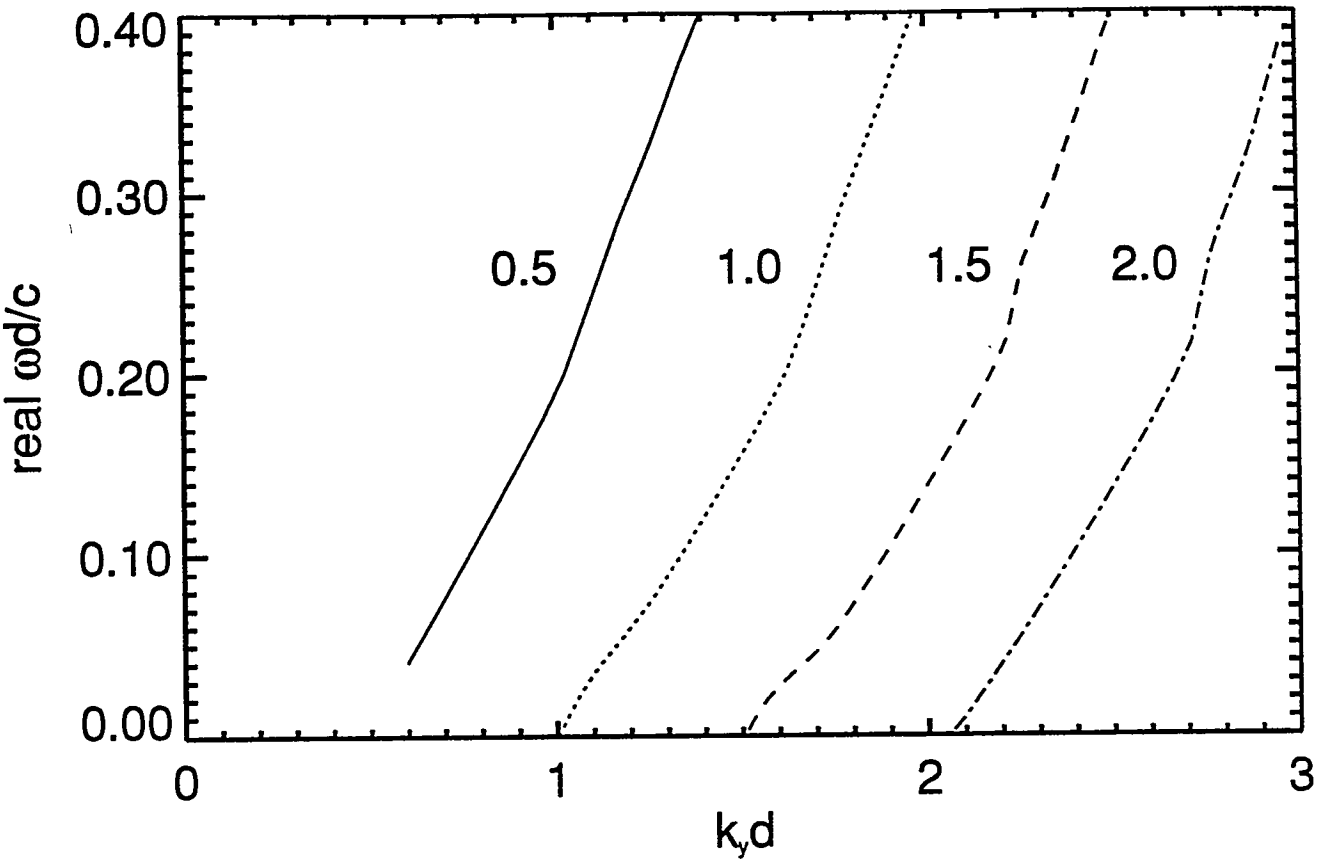
0.40
0.30
0.20
0.10
0.00
real ωd/c
0.5
1.0
1.5
2.0
0
1
2
3
k_y d

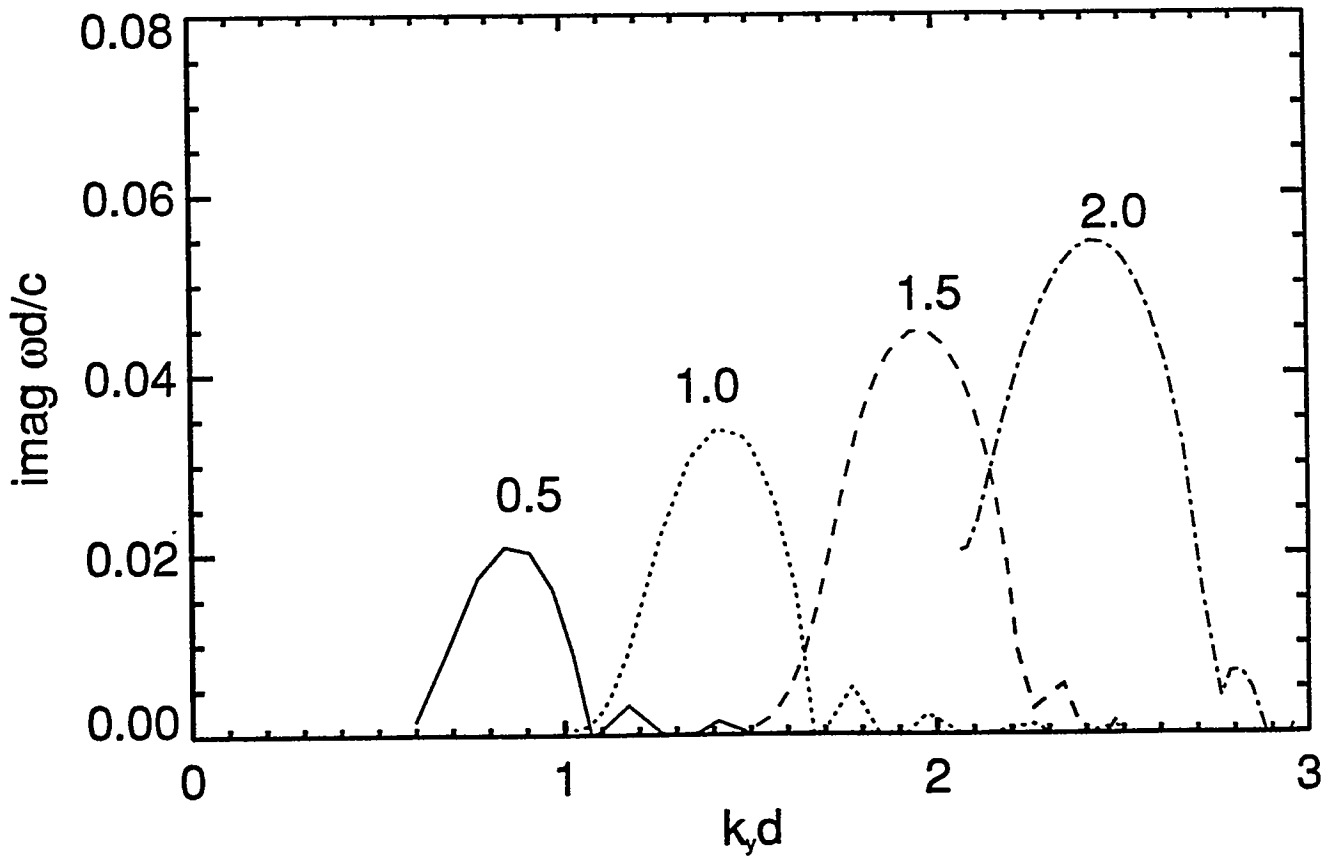
0.08
0.06
0.04
0.02
0.00
imag ωd/c
0.5
1.0
1.5
2.0
0
1
2
3
k_y d

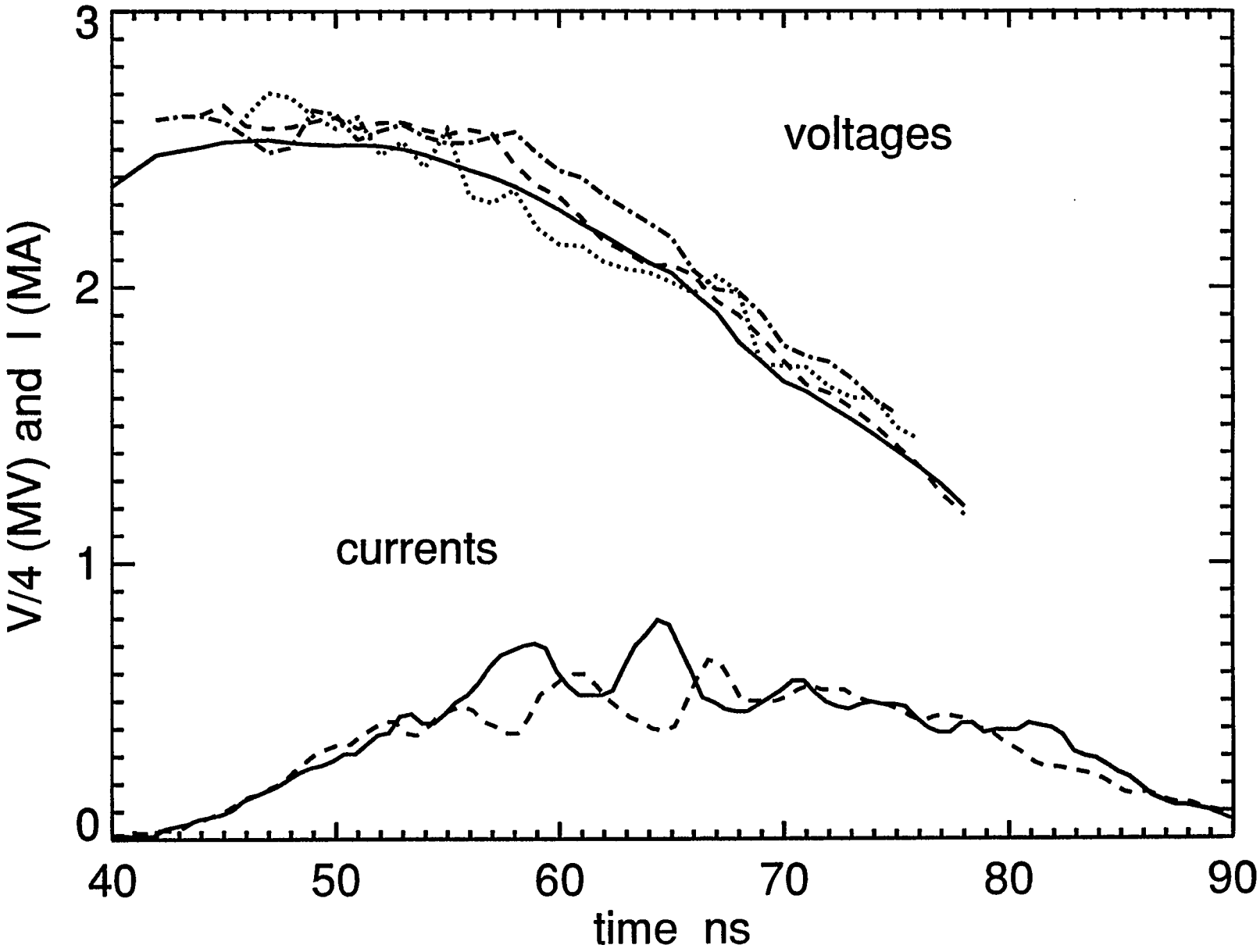
3
2
1
0
V/4 (MV) and I (MA)
voltages
currents
40
50
60
70
80
90
time ns

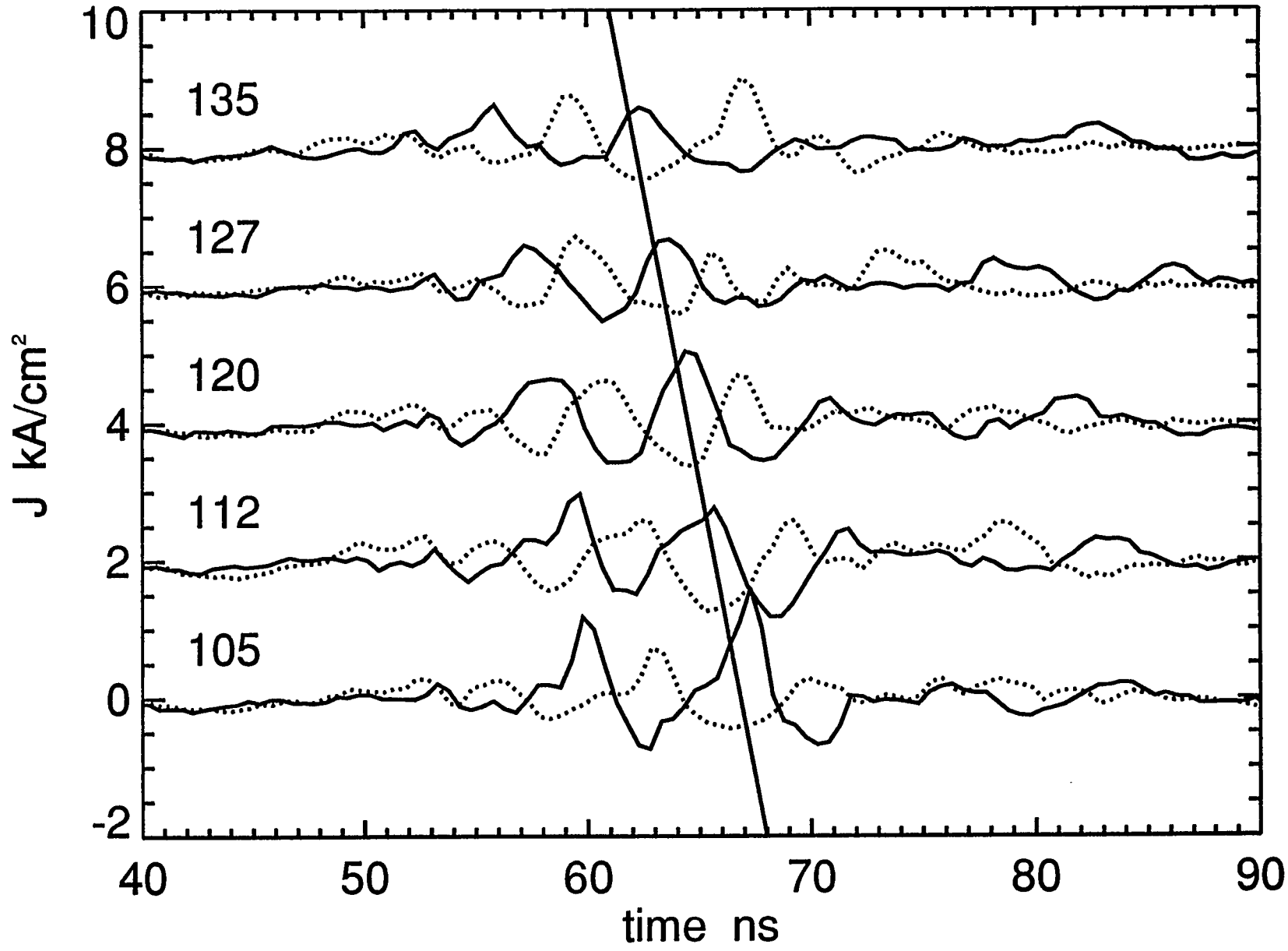
10
8
6
4
2
0
-2
135
127
120
112
105
J kA/cm²
40
50
60
70
80
90
time ns

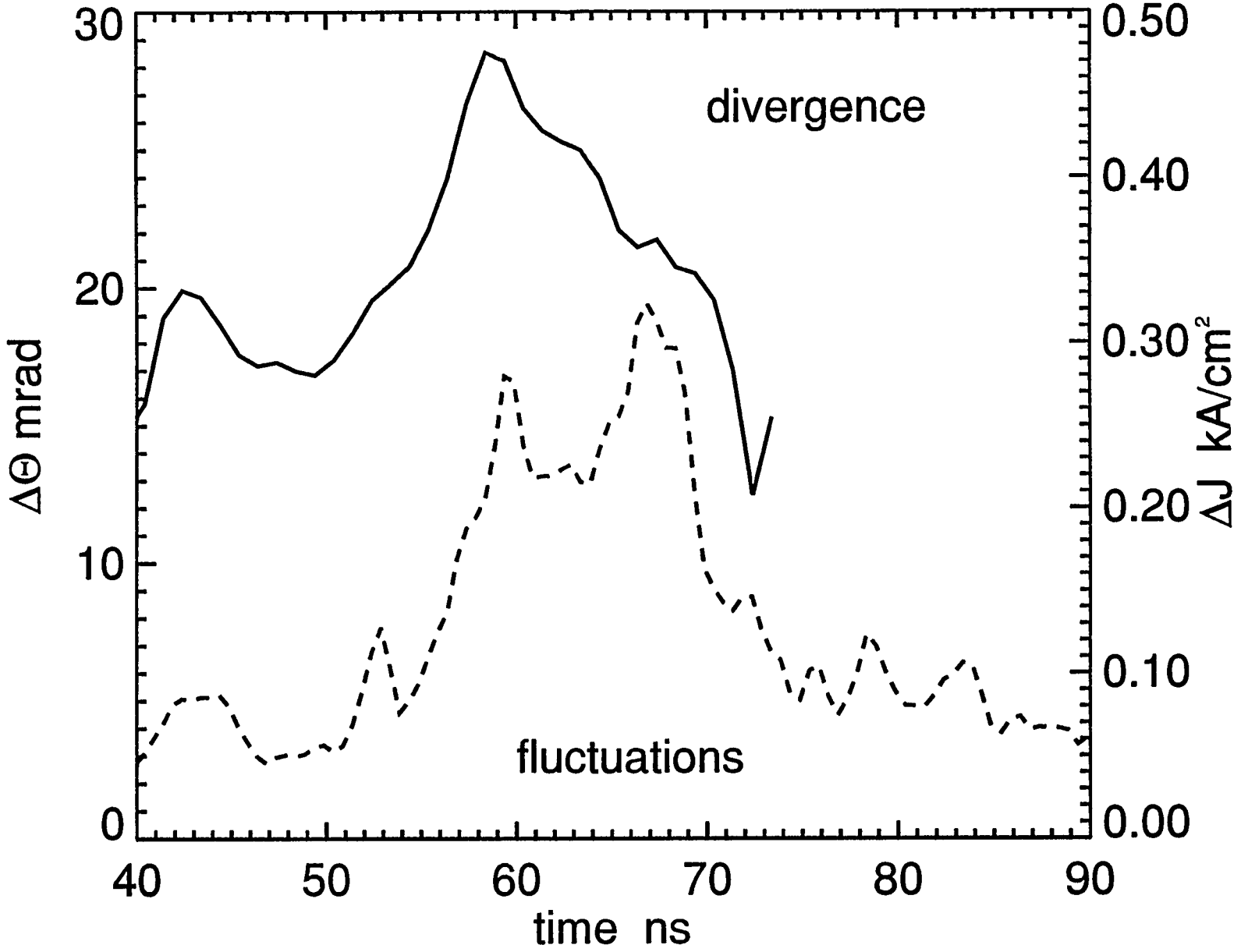
30
20
10
0
0.50
0.40
0.30
0.20
0.10
0.00
ΔΘ mrad
ΔJ kA/cm²
divergence
fluctuations
40
50
60
70
80
90
time ns

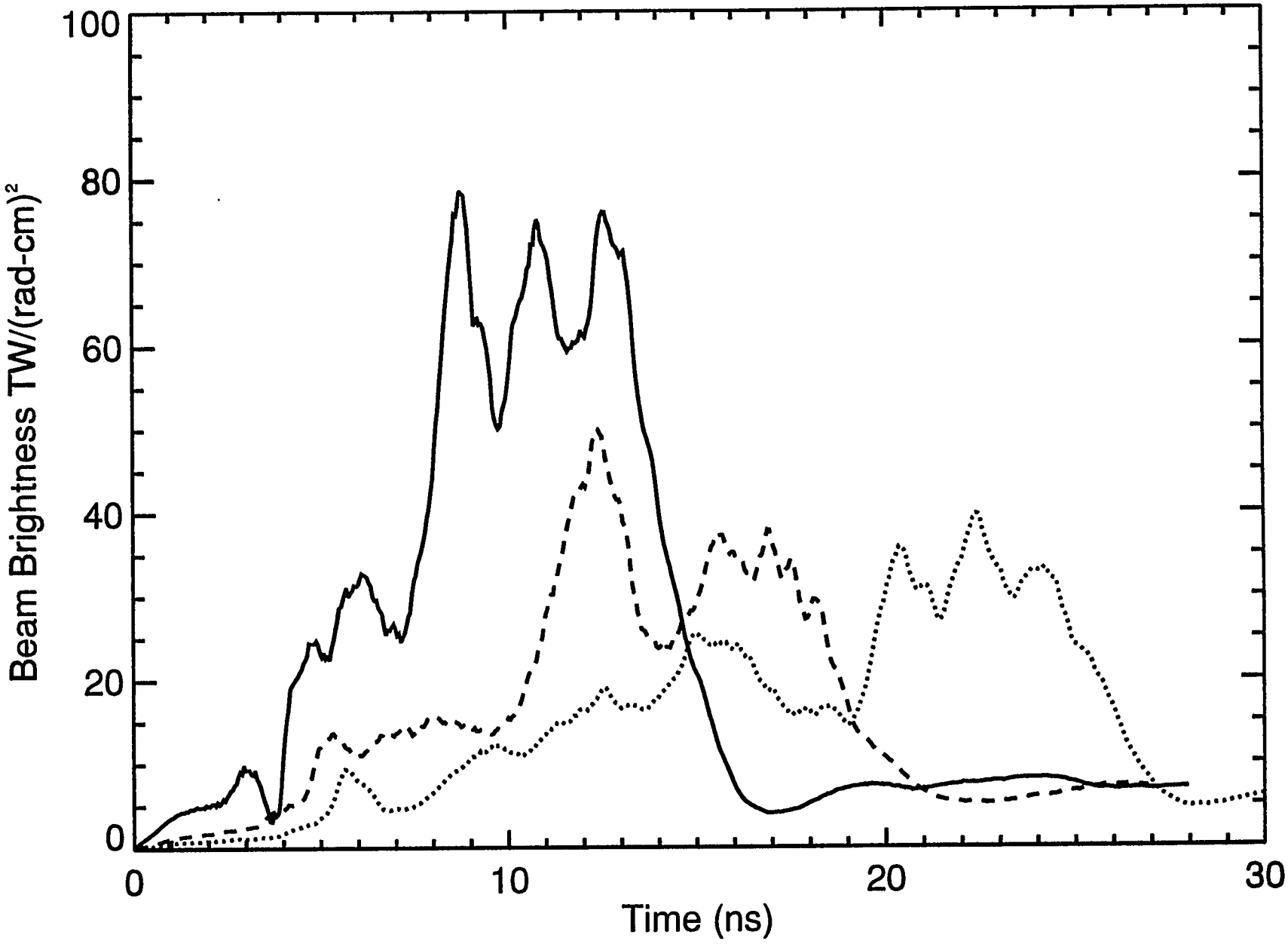
100
80
60
40
20
0
Beam Brightness TW/(rad-cm)²
0
10
20
30
Time (ns)